REVIEW

Check for updates

Recent progress in nanomedicine-mediated cytosolic delivery

Hangyu Son, [ID] Jeongsu Shin [ID] and Joonhyuck Park [ID] *

Cytosolic delivery of bioactive agents has exhibited great potential to cure undruggable targets and diseases. Because biological cell membranes are a natural barrier for living cells, efficient delivery methods are required to transfer bioactive and therapeutic agents into the cytosol. Various strategies that do not require cell invasive and harmful processes, such as endosomal escape, cell-penetrating peptides, stimuli-sensitive delivery, and fusogenic liposomes, have been developed for cytosolic delivery. Nanoparticles can easily display functionalization ligands on their surfaces, enabling many bio-applications for cytosolic delivery of various cargo, including genes, proteins, and small-molecule drugs. Cytosolic delivery uses nanoparticle-based delivery systems to avoid degradation of proteins and keep the functionality of other bioactive molecules, and functionalization of nanoparticle-based delivery vehicles imparts a specific targeting ability. With these advantages, nanomedicines have been used for organelle-specific tagging, vaccine delivery for enhanced immunotherapy, and intracellular delivery of proteins and genes. Optimization of the size, surface charges, specific targeting ability, and composition of nanoparticles is needed for various cargos and target cells. Toxicity issues with the nanoparticle material must be managed to enable clinical use.

1 Introduction

Nanomedicine is known to use sub-micrometer-sized delivery vehicles to transport various bioactive molecules and proteins.[1–3] Proteins and genes are the most important components for the structure, regulation, and biological function of the body.[4] Malfunction or mutation of those components often leads to a detrimental status and incurable diseases.

Department of Medical Life Sciences, Department of Biomedicine & Health Sciences, College of Medicine, The Catholic University of Korea, 222 Banpo-daero, Seocho-gu, Seoul, 06591, Republic of Korea. E-mail: joonpark@catholic.ac.kr

When proteins are damaged, direct replacement and regulation of downstream signaling pathways *via* agonistic protein–protein interactions can be a straightforward therapeutic strategy.[5] Microinjection, electroporation, and sonoporation are physical delivery methods.[6–9] However, those traditional methods for transient permeabilization through physical delivery are low-throughput and invasive, potentially causing side effects and hindering cell function. For transient protein delivery, an antibody is the most popular bioactive protein due to its excellent targeting ability and selectivity. The US Food and Drug Administration (FDA) has approved more than 10 types of antibody-drug conjugates for clinical use.[10] However, they

Hangyu Son obtained his B.S. from Hannam University. Currently, he is a graduate student under the supervision of Prof. Joonhyuck Park in the Department of Biomedical and Health Sciences at The Catholic University of Korea. His research interests are focused on the drug delivery system and biosensors via inorganic nanoparticles. He anticipates that he can contribute novel therapeutic field of nanomedicine.

Jeongsu Shin obtained his B.S. from the Kangwon University. Currently, he is a graduate student under the supervision of Prof. Joonhyuck Park in the Department of Biomedical and Health Sciences at The Catholic University of Korea. His research interests are focused on the drug delivery system and biosensors.

mainly target secreted or cell membrane proteins. Exogenous gene delivery *via* a viral carrier or plasmid can insert genetic information, but that can have harmful effects, including potential oncogenesis.[11] Even though many small-molecule and water-soluble drugs can inhibit endogenous enzymes inside the cell cytosol or organelles, their low-efficiency intracellular delivery and rapid clearance from *in vivo* systems make them unsuitable for clinical use.[12,13]

To address those issues, cytosolic delivery of nanomedicines carrying proteins, genes, and small-molecule drugs has become attractive.[14] Tailoring the surface chemistry of nanoparticles (NPs) provides enhanced colloidal stability and the ability to deliver cargo proteins directly to the cytosol. NP-based carrier platforms use electrostatic interactions to form complexes between a nanocarrier and its cargo proteins.[15–18] When the cargo biomolecule is a gene, the nanomedicine delivery system protects the gene from digestion enzyme activity and other unfavorable conditions during *in vivo* delivery. Also, small molecules usually exhibit rapid pharmacokinetics, so a massive amount or a suspended release system is often required for curing diseases.[19]

Despite the importance of bioactive proteins and genes, direct cytosolic delivery of cargo biomolecules remains challenging because the lipid bilayer has an inherent negative charge that repels most proteins and genes. Penetration of the lipid bilayer barrier requires secure colloidal stability of the delivery vehicle in a hydrophilic environment. Custom-designed nanomachines can penetrate through the hydrophobic part of the lipid bilayer.[20] However, a delivery strategy versatile enough to carry various types of biomolecules and drugs is needed.

Delivery strategies for nanomedicine, including cell-penetrating peptide (CPP)-mediated delivery, endosomal escape, stimuli-sensitive delivery, and fusogenic liposomes (FLs), have been studied extensively. In 1988, researchers found that the transactivator of the transcription (TAT) protein of HIV-1 played a key role in transporting viral genetic information through the cell membrane.[21] CPPs are usually composed of 5 to 30 amino acids and can be internalized into cells *via* various

delivery mechanisms. The surface of a nanomedicine can be tethered by cationic or amphiphilic CPPs, resulting in direct cytosolic delivery.[22–24] However, the mechanism for cytosolic delivery using CPPs is not fully understood and often requires both direct cytosol and endocytic delivery. Endosomal escape *via* the proton sponge effect is normally assisted by protonable cationic polymers.[25] Proton influx from the cytosol to the endosome increases the concentration of the counterion until the osmotic pressure becomes high enough to disturb the structural stability of the endosome. Fusion or pore formation in the endosomal membrane also is proposed. During endocytosis, the cargo biomolecules are exposed to acidic pH, which destroys their enzymatic activity and the 3D structure of natural proteins.[26] The low efficiency of endosomal escape is another issue with this drug-delivery method. Stimuli-sensitive delivery methods are widely accepted in various drug delivery fields.[27,28] The cytosolic delivery of bioactive cargos encapsulated in a nanomedicine can happen under many different cues from certain cell lines or tissues. As the stimulus for cargo delivery, pH, hypoxia, and near-infrared (NIR) light have been used. In a mouse model and in clinical use, these stimuli-sensitive methods are essential to decreasing off-target activity and increasing the efficiency of cytosolic delivery. FLs are spherical vesicles composed of a single or bilayer of lipids.[29] The components of a FL are mostly cationic and amphiphilic lipids. The delivery mechanism of FLs remains elusive. Membrane fusion and endocytosis are possible major delivery mechanisms, and both methods disturb the host lipids. The nanomedicine and cell type for each experiment must be chosen carefully.

Here, we focus on recent progress in the cytosolic delivery of nanomedicines, including various delivery strategies (penetrating peptides, endosomal escape, stimuli-sensitive delivery, fusogenic liposomes), their delivery mechanisms, and applications (Scheme 1). Depending on their delivery methods and mechanisms, we introduce nanomedicines for cytosolic delivery that have been applied in organelle-specific tagging, vaccine delivery for enhanced immunotherapy, and intracellular delivery of bioactive molecules. This review also described the commercialized or clinically tested nanomedicine adopting the cytosolic delivery methods. Finally, we mention future perspectives on what aspects are needed to be carefully considered and customized to achieve clinically applicable nanomedicines through cytosolic delivery.

Joonhyuck Park received his B.S. and PhD in chemistry from Pohang University of Science and Technology (POSTECH) and trained as a postdoctoral researcher at University of California, Los Angeles (UCLA) and University of Illinois at Urbana-Champaign (UIUC). Now, he is an assistant professor at the Department of Medical Life Sciences in the College of Medicine, The Catholic University of Korea. His research goal is developing nanomaterials that can be applied to therapy and imaging. He is interested in nanocrystals with new optical/physical/chemical properties and their applications at the nano-bio interfaces.
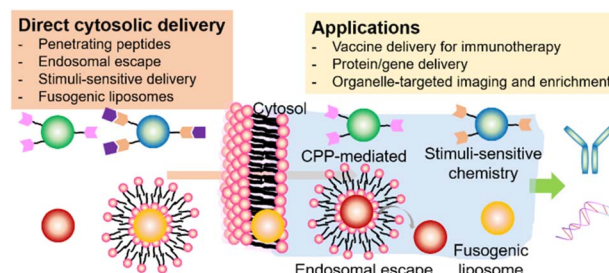
Scheme 1 Schematic representation of the nanomedicine-mediated cytosolic delivery.

2 Delivery methods

2.1 Penetrating peptides

Major obstacles to protein therapy are low membrane penetration and endosomal entrapment of cargo proteins. To address these issues, CPPs have been used as functional groups on nanoparticles, which can delivered into the cytosol under various mechanisms (Scheme 2). The target proteins can be encapsulated by a CPP-modified NP or formed by mixing CPPs and target proteins *via* electrostatic interaction. Liyi Fu *et al.* developed multistage NPs that were activated by a tumor microenvironment (Fig. 1).[30] They produced MPEG-PHMEMA NPs out of both a hydrophilic block (methoxy poly(ethylene glycol) (MPEG)) and a hydrophobic block (poly(2-(hexamethyleneimino)ethyl methacrylate) (PHMEMA)) containing tetraguanidinium-modified saporin (TG-S). Saporin is a ribosome-inactivating protein and was encapsulated inside the NPs. The MPEG-PHMEMA NPs had a hydrodynamic (HD) size of 80 nm at pH 7.4 and released TG-S at pH 6.5, which is a tumor microenvironment condition. Efficient and direct cytosolic delivery of green fluorescent protein (GFP) or dye-labeled saporin-loaded NPs to A549 cells and spheroid cells was confirmed by confocal laser scanning microscopy (CLSM). The antitumor effect of the TG-S-loaded MPEG-PHMEMA NPs was confirmed in an A549 xenograft mouse model.

Easy complexation between CPP-functionalized carriers and cargo proteins has been applied to cytosolic delivery of proteins. Lv *et al.* synthesized guanidyl-functionalized polyethyleneimine (PEI) that can be used as a protein carrier and a protonable
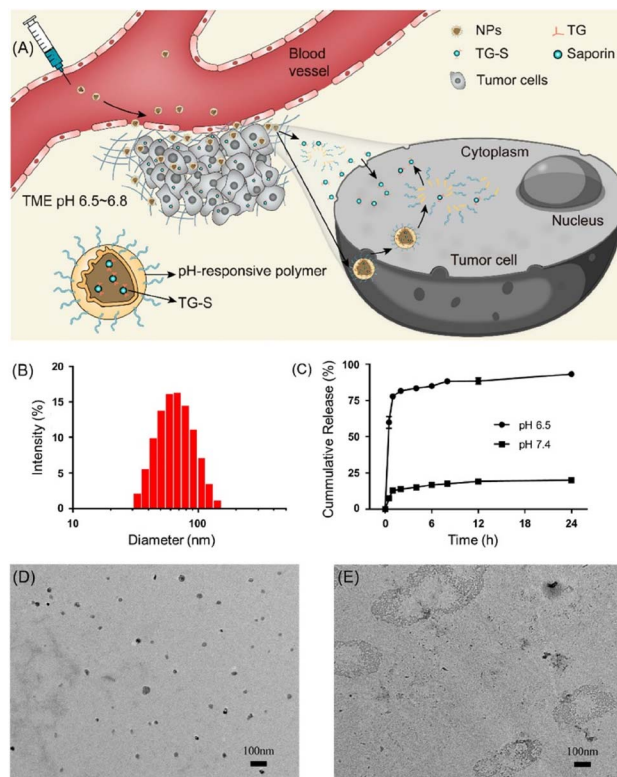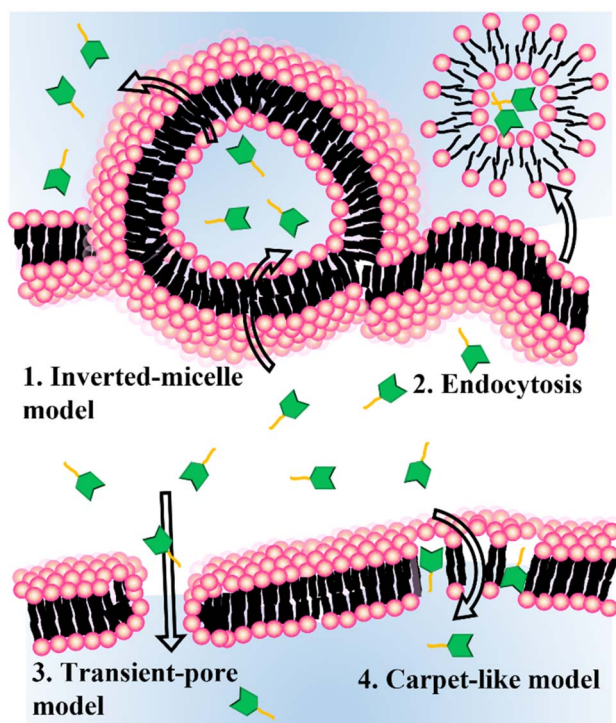

Fig. 1 Tumor microenvironment dependent cytosolic delivery of MPEG-PHMEMA-NPs which encapsulate tetraguanidinium and model protein. This figure has been reproduced from ref. 30 with permission from [American Chemical Society], copyright [2022].

Scheme 2 Schematic representation of cytosolic delivery mechanisms for the cell-penetrating peptides.

polymer for endosomal escape.[31] The guanidyl group can interact with residual groups of proteins through the salt bridge and hydrogen bonding. With those interactions, the guanidyl-rich PEIs delivered various types of protein (bovine serum albumin, beta-galactosidase, horseradish peroxidase, chymotrypsin, and trypsin) while preserving their bioactivity. Among the 18 guanidyl-rich polymers tested, 4-guanodinobenzoic acid (GBA)-functionalized PEIs exhibited the most efficient delivery of cargo proteins. The complex has an HD size of 200–300 nm and is positively charged. The complexes were colloidally stable under buffer conditions and efficiently delivered their cargo proteins through charge interaction between the guanidyl groups and negatively charged biomolecules on the cell membrane. The authors claimed that the colloidal stability might have originated from paired guanidyl-π interactions between the benzene and guanidyl groups. While cytosolic delivery of the cargo was demonstrated, an endocytosis mechanism study of GBA-coated PEIs revealed that delivery of cargo proteins also followed energy-dependent endocytosis along multiple pathways.

Genetic manipulation of protein expression and purification has been used for cytosolic delivery for decades because natural proteins normally cannot be delivered into the cytoplasm. However, post-modification of natural proteins has been studied by researchers because of its easy and simple processes. Kitagishi *et al.* achieved efficient cytosolic delivery of proteins

and liposomes using host–guest chemistry, which uses non-covalent supramolecule interactions between β-cyclodextrin (CD, host) and adamantane (Ad, guest).[32] They used click chemistry between the octaarginine (R8) chain and CD to achieve cell-penetrating CD (R8-CD^{OH}). They then used non-covalent interactions to obtain a complex of the R8-CD^{OH} carrier and Ad tagging molecules. Based on the cationic charge of the R8, the R8-CD^{OH} carriers can be delivered directly into the cytosol. CD exhibits water solubility, low cytotoxicity, and biocompatibility. Because the Ad tags tethered on the cargo protein (GFP, β-gal, and IgG) are very small, they had no noticeable effect on the structure or function of the cargo proteins. Furthermore, the Ad tags are easy to modify on amine groups of the protein via the N-hydroxysuccinimide reaction.

Proteins play a pivotal role in signal transduction and cellular homeostasis, and abnormal proteins can cause serious disease. Mout et al. reported direct cytosolic delivery using proteins with an oligo(glutamate) sequence (E-tag) and arginine-terminalized gold NPs (ArgNPs).[33] Nanoassemblies (HD size: ~500 nm) can be formed by mixing the E-tagged cargo proteins and ArgNPs (HD size: 10 nm) via electrostatic interactions. Specifically, E-tagged granzyme A, which can induce apoptosis, was delivered to the cytosol of HeLa cells. That same research group reported an ArgNP delivery system that used nanovectors to deliver biotinylated proteins through the biotin-streptavidin interaction (Fig. 2).[34] Those biologically self-assembled complexes were achieved by mixing biotinylated cargo proteins poly(oxanorbornene)imide polymers (PONI-Guan) was added to the STV/b-E20/b-proteins, producing self-assembled nanocomposites (HD size: 200–350 nm) of STV/b-E20/b-protein and PONI-Guan via electrostatic interaction. The cytosolic delivery of the nanocomposites was similar to that with the ArgNP-based delivery mechanism: which was directly delivered into the cytosol by membrane fusion-like manners by E-tagging. GFP and granzyme A were used as cargo proteins, and fluorescence images and cell apoptosis for GFP and granzyme A, respectively, were confirmed under CLSM. CPPs have been also applied in a delivery of drugs,[35] viral particles[36] and semiconductor nanoparticles.[37]

2.2 Endosomal escape

Cytosolic delivery has a unique benefit when the target proteins or subcellular organelles are located inside cells, which generally makes them undruggable and/or unreachable by the protein or drug itself. Among the cytosolic delivery methods, endosomal escape has been investigated by many researchers. Ren et al. introduced a dendrimer delivery platform that was functionalized with dipicolylamine (DPA).[38] The DPA moieties can bind to Zn^{2+} ions through a coordination bond, and further coordination can be achieved by anionic (sulfate, phosphate, and carboxyl groups), cationic (imidazole and amines), and hydrophobic functional groups. An amine-terminated poly-amidoamine dendrimer was functionalized with DPA and termed GD. It had an HD size of ~150 nm and high delivery efficiency when 57 DPA ligands were tethered on its outmost surface. Those authors claimed that endosomal escape occurred due to the excellent pH-buffering capability of the DPA/Zn^{2+}. The endocytosis mechanism of GD was mainly governed by micropinocytosis-dependent and lipid-raft-mediated pathways. Other metal ions (Cu^{2+}, Mn^{2+}, Fe^{2+}, Ni^{2+}, Co^{2+}) were used instead of Zn^{2+}, but Cu^{2+} showed only about half the delivery efficiency of Zn^{2+}. CLSM confirmed the efficient delivery of fluorescein 5-isothiocyanate (FITC)-conjugated bovine serum albumin and 5–10 oligopeptides using the dendrimer carrier system.

He et al. introduced an endosomal escape strategy by a particle-to-fiber transition (Fig. 3). They showcased the efficient cytosolic delivery and endosomal escape of phosphopeptides or alkaline phosphatase (ALP).[39] ALP is located in lipid rafts and catalyzes dephosphorylation when phosphopeptides are localized on the cell membrane. The phosphopeptides then self-assemble with one another. The researchers synthesized
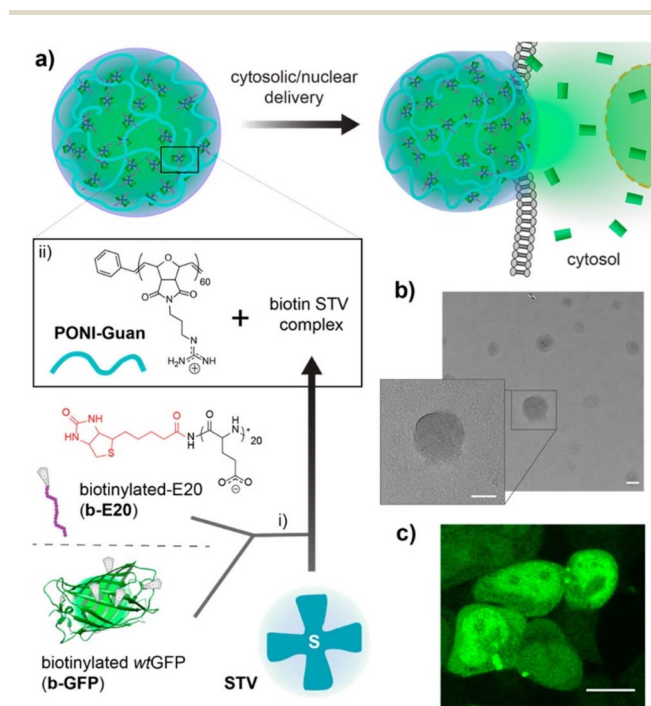

Fig. 2 Schematic representation of preparing guanidinium-functionalized polymer and streptavidin nanocomposites with biotinylated cargos. This figure has been reproduced from ref. 34 with permission from [American Chemical Society], copyright [2022].
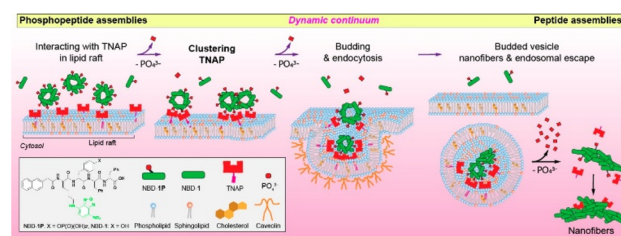

Fig. 3 Illustration how endosomal escape occurred by making nanofibers which consequence of interaction with phosphoprotein and TNAP. This figure has been reproduced from ref. 39 with permission from [American Chemical Society], copyright [2021].

a fluorescent phosphopeptide (NBD-1p) using nitro-benzoxadiazole (NBD) as the fluorophore and naphthyl-conjugated D-phosphotetrapeptide (D-Lys-D-pTyr-D-Phe-D-Phe) as the phosphopeptide. They confirmed their hypothesis using HEK293 cells that overexpressed a red-fluorescent protein tag on a tissue-nonspecific alkaline phosphatase (TNAP). The NBD-1p was localized on the cellular membrane and interacted with the TNAP by the dephosphorylation. When the NBD-1p assembled properly, endocytosis occurred, and the TNAP was endocytosed. In the endosome, the NBD-1p assemblies were dephosphorylated continuously, forming a nanofiber with an HD size of 300–1000 nm. Those nanofibers ruptured the endosome, resulting in cytosolic delivery of the cargo.

Beach *et al.* reported the sensitive and quantitative determination method of luciferase endosomal escape to estimate the efficiency of endosomal escape.[40] Poly(2-diethylamino ethyl methacrylate) (PDEAEMA) and poly(2-diisopropylamino ethyl methacrylate) (PDPAEMA) were used as protonable polymers that can be protonated on amine moieties under acidic pH. The protonation process induced disassembly of NPs and endosomal escape through a build-up of osmotic pressure. The core PDPAEMA (pK_a: 5.6) and PDEAEMA-*r*-PDPAEMA (pK_a: 6.4) polymers were used as the carrier for delivery. The *in situ* biolumi-nescent pair (LgBiT (17.8 kDa) and HiBiT (1.3 kDa)) was used as a signal reporter when the polymer carrier was delivered into the cytosol. LgBiT was expressed in the cytosol of HEK293T cells, and HiBiT peptides were conjugated on the core polymer. When endosomal escape occurred, the LgBiT met the HiBiT, and a luminescent signal was produced. Those authors claimed that the concentration of core polymer-based carrier they used did not induce full disruption of the endosome but only a partial puncture that resulted in diffusion of cargo protein from the endosome to the cytosol without noticeable cytotoxicity.

2.3 Stimuli-sensitive delivery

Carriers with high serum tolerance are needed for efficient cytosolic delivery systems *in vivo* because complexes assembled through electrostatic interaction are labile under physiological conditions. Zhang *et al.* created pH-responsive G5-DAITC (GDA) composed of a generation-five PAMAM dendrimer (G5) and 4-diethylaminophenyl isothiocyanate (DAITC).[41] GDAs with a high proportion of DAITC (pK_a: 4.7) retained their shape at physiological pH and completely disassembled at endolysosomal pH. The GDA/enhanced green fluorescent protein (EGFP) complexes had an HD size around 253 nm and released about 20% of their EGFP in serum-containing medium and all of it at a pH lower than 6.0. The complexes were able to enter cells through lipid-raft-mediated and clathrin-mediated endocytosis. Those authors used flow cytometry to investigate whether the GDA protected the native function of ribonuclease A (RNase A) and found that the GDA did protect the enzymatic function of RNase A (>60% cell apoptosis was induced). GDA successfully transported diverse cargo, including FITC-labeled RNase A, oval-bumin, α-chymotrypsin, superoxide dismutase, rhodamine B isothiocyanate-labeled catalase, yellow fluorescent protein, and R-phycoerythrin, into 143B cells and other cell types.

To knock down oncogenes, oligonucleotide drugs (ONDs) have been used as an anticancer medicine. The biggest draw-back of ONDs is that they are effortlessly degraded by endoge-nous nucleases and are difficult to load into the cytoplasm with a negative charge. Chen *et al.* reported a photolabile spherical nucleic acid (PSNA) as a delivery carrier (Fig. 4).[42] They used two-step NIR light illumination to control the disassembly of PSNA and activate gene therapy with photodynamic therapy. The PSNA was composed of an amphiphilic OND, a singlet oxygen-degradable linker, pheophorbide a, hydrophilic siRNA, and hydrophobic peptide nucleic acid–based antisense oligonucle-otide (pASO). After light irradiation, the PSNA structure was disrupted, and the HD size increased from 126 nm, which did not occur in the negative control. Cellular uptake of PSNA was observed in HeLa cells using Cy3-labeled siRNA[H], Cy7-labeled pASO[B], and a lysosome tracker, with 90% overlap between the siRNA and the lysosome tracker. Upon illumination with 670 nm light, the HIF-1a and Bcl-2 expression levels, which were selected as the targets for gene therapy, were significantly downregulated in a dose- and irradiation time-dependent manner, reducing the cell viability by almost 31%.

Sloand *et al.* applied perfluorocarbon (PFC) nanoemulsion carriers of protein biotherapeutics for cytosolic delivery *via* ultrasound (US) activation. The PFC nanoemulsions are note-worthy stimulus-responsive delivery carriers with clinical applications.[43] However, they suffer strong hydrophobicity caused by their fluorous liquid interior. Those authors created ionic perfluorononanoic acid (PFNA), which was composed of perfluorohexane and fluorous tags and had the capacity for fluorous masking and counterbalancing against the polarity of fluorine content. The PFNA can be applied for US-mediated cytosolic transduction. They confirmed the ability of the fluo-rous nanoemulsions to allow on-demand cytosolic delivery of
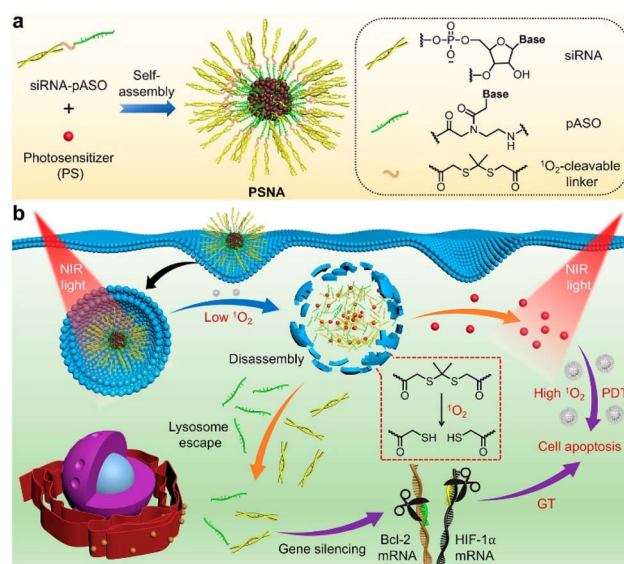

Fig. 4 Schematic representation for the design of photolabile spherical nucleic acid (PSNA). This figure has been reproduced from ref. 42 with permission from [American Chemical Society], copyright [2021].

biological cargo under US activation. Then, they constructed perfluoropentane-based peptide emulsions (NE$_{GFP}$) that were encapsulated by a peptide emulsifier with a sequence specific for the cell-targeted fluorous nanoemulsions with an HD size of ∼300 nm. The NE$_{GFP}$ showed rapid transduction of GFP into human A549 cells after the US trigger, whereas no detection of GFP was observed before the trigger. Purified rabbit IgG (∼150 kDa) was used, and the NE$_{IgG}$ particles facilitated on-demand and transiently controlled intracellular delivery of the cargo upon US activation. They used a human HRas^{G12V}-expressing mouse, susceptible to cutaneous squamous papillomas, to test the *in vivo* applicability of the nanoemulsions, and they found that the NE$_{IgG}$ successfully permeated the tissue under an external US pulse.

RNase has gained great attention because it is a high efficacy, high specificity anti-cancer agent. However, natural RNase has high instability, a short lifespan, and deficient membrane permeabilization. Si *et al.* introduced the supramolecular nanogels which deliver RNase safely.[44] The nanogels were synthesized using one of two block copolymers, either azobenzene (Azo) or β-cyclodextrin (βCD) conjugated with poly(ʟ-glutamic acid)-*graft*-poly(ethylene glycol) methyl ester (PLG-*g*-mPEG), to produce PLG-*g*-mPEG/Azo or PLG-*g*-mPEG/βCD, respectively. Through their host–guest interaction, RNase was encapsulated inside the nanogels in an aqueous condition (Nano-RNase). The HD size of this complex was 126 nm. Along with nitroreductase (NTR), which is highly expressed in hypoxic tumor sites, the non-covalent interactions in Azo and βCD become labile, which releases the RNase. Using FITC-labeled RNase, the authors demonstrated efficient cytosolic delivery and death rate of 4T1 tumor cells and showed tumor suppression in 4T1-tumor-bearing mice. The endocytosis mechanism of the nanogels was confirmed to be energy-dependent and to occur along multiple pathways.

2.4 Fusogenic liposomes

Even though the hepatitis B virus (HBV) causes a crucial disease, it is a challenge to treat efficiently due to drug resistance and the adverse events of present treatments. Most NP uptake is accomplished by endocytosis, which leaves the NPs entrapped in the endosomal compartments and inhibits their direct delivery interaction with the cytosol and organelles. Therefore, NPs that can bypass the endosome are needed for intracellular cytosolic delivery and organelle manipulation.

Hu *et al.* used membrane fusion strategy to transfer hepatitis B surface antigen (HBsAg) into the cytoplasm (Fig. 5).[45] They created liposomes of 1,2-dioleoyl-*sn*-glycero-3-phosphoethanolamine (DOPE), CpG, cholesteryl hemisuccinate, and HBsAg (HBsAg&CpG@Lip) that possessed pH responsiveness and had an HD size of ∼195 nm. Interestingly, their size could be increased to 790 nm in an acidic environment, whereas it did not change under a neutral pH. The liposome containing HBsAg increased the amount of antigen uptake without noteworthy cytotoxicity compared with the unaccompanied antigen. Additionally, it improved the MHC II, TNF-a, CD86, and CD40 expression levels on bone marrow-
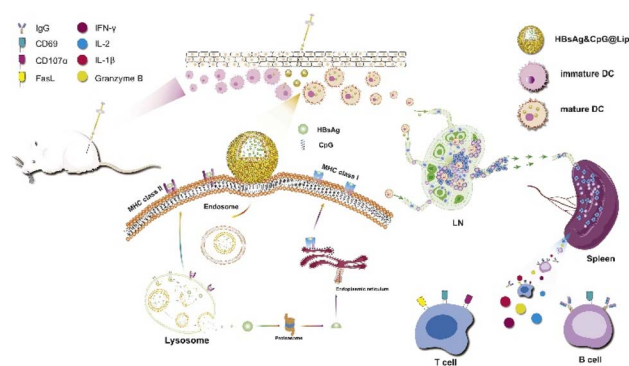

Fig. 5 Schematic representation of the immunization process, including antigen uptake/activation, the cytosolic release of HBsAg for subsequent cross-presentation, and the activation of lymph nodes and immune responses. This figure has been reproduced from ref. 45 with permission from [Elsevier], copyright [2020].

derived dendritic cells (BMDCs). HBsAg was colocalized with the lysosomes in BMDCs. When the liposomes were injected into the legs of Balb/c mice, the expression of MHC I and II, CD40, and CD86 increased. The expression of CD69 and CD27 was enhanced when C57BL/6 mice were inoculated with the HBsAg&CpG@Lip. The HBsAg&CpG@Lip could encourage the proliferation of IFN-γ-secreting cells and the expression of CD69 on the surfaces of T cells, both of which are required to activate cytotoxic T lymphocytes.

Chen *et al.* presented cell membrane FLs that enabled cytosolic delivery of proteins and nanoparticles.[46] They used magnetic NPs (MNPs) coated with positively charged FLs produced with 1,2-dimyristoyl-*sn*-glycero-3-phosphocholine (DMPC), 1,2-distearoyl-*sn*-glycero-3-phosphoethanolamine-poly(ethylene glycol) (DSPE-PEG), and 1,2-dioleoyl-3-(trimethylammonium)propane (DOTAP) at the molar ratio of 76.2 : 3.8 : 20, respectively. The bare MNP HD size was 61 nm, and the final HD size of the lipo-MNPs was around 200 nm. To determine whether the uptake of lipo-MNPs depended on membrane fusion, they administered lipo-MNPs to ARPE-19 cells, which were preincubated with the membrane fusion inhibitor, enfuvirtide. They found that the liposomes and MNPs were completely inhibited. After internalization, only a few of the MNPs colocalized with the liposomes and early endosomes. Therefore, most of the fusogenic MNPs permeated the cells through liposome-membrane fusion. With the addition of the lysosome-targeting Lamp1-GFP, enhanced lysosome localization of MNPs was confirmed.

Positively charged FLs have been widely used to deliver cargo through the cellular membrane. Because the net charge of a cellular membrane is usually negative, negatively charged cargo, such as DNA, mRNA, and siRNA, hampers the interaction between FLs and the cellular membrane. As the amount of negatively charged cargo increases, the cytosolic delivery efficiency of FLs can be lowered. Hoffmann *et al.* reported an optimized amount of neutralization reagent (NR) and liposome compositions for nucleic acid (NA) transfection because the partial neutralization of NAs improves their delivery efficiency

by membrane fusion.[47] The optimal molar ratio of NR/siRNA, mRNA, and pDNA was 5/1, 50/1, and 450/1, respectively. Those authors claimed that the FL/NR complexes with the highest zeta potential showed the highest mRNA transfection efficiency. Their DOPE/DOTAP/1,1-dioctadecyl-3,3,3,3-tetramethylindotricarbocyanine (DIR) (1/1/0.1) FLs can cause 1700 fusions per cell within 10 minutes, resulting in the movement of nearly 10^5 mRNA molecules per cell into the cytoplasm. Because the primary tissue is one of the hardest cells to transfer, FL/NR/NA complexes were administered to primary cortical tissue and isolated rat embryonic cortical tissue for mRNA delivery, and high-efficiency transfection of eGFP-mRNA to primary tissues was detected.

3 Applications

3.1 Vaccine delivery for immunotherapy

Cancer immunotherapy (CIT) encourages the immune system to attack cancerous tissues and cells by controlling the immune microenvironment. Cyclic-GMP-AMP (cGAMP) that can activate the stimulator of the interferon gene has been considered an important factor in initiating anticancer immunity. Because cGAMP is an inherently unstable small molecule that shows fast clearance, its intracellular delivery efficiency is very low. Chen *et al.* reported a redox-responsible cGAMP-loaded nanovaccine (NV) composed of an arginine-modified disulfide monomer, cGAMP, and Mn^{2+} ions (Fig. 6).[48] It was 176 nm in diameter and released cGAMP in a physiological reducing environment. Mn^{2+} ions stabilized the NV structure, and the disulfide monomer formed polysulfides. Disassembly of the polysulfides under physiological conditions was confirmed and allowed direct cytosolic delivery of the NV. Flow cytometry and ELISA for cytokines confirmed that administration of Mn-cGAMP NV led to the maturation of bone marrow-derived dendritic cells. The immunostimulatory potency of the Mn-cGAMP NV was similar to that of the LPS used as the positive control. Intratumoral injection of the Mn-cGAMP NV suppressed the tumor growth rate and improved the survival rate of mice in a B16F10 tumor

xenograft model by recruiting both CD3 and CD8 T cells. The lymph nodes and spleen were effectively activated (2–3 times more mature DCs and mass of spleen) and delayed tumor growth. Cytosolic delivery of cGAMP NV was demonstrated as an NP-based small-molecule delivery system that resulted in effective CIT.

Myocardial infarction (MI) causes acute inflammation and recruits immune cells rapidly, causing tissue damage and heart failure. Immune tolerance for antigens from damaged MI tissue can limit excess inflammation. Kwon *et al.* reported an NP-based vaccine composed of MI tissue lysate (antigen), unilamellar liposome, and rapamycin (L-Ag/R).[49] After MI, MI tissue lysate can be used as specific antigens to induce immune responses. When the MI tissue lysate was administered with the loaded rapamycin, it reduced pro-inflammatory cytokines (IL-1, IL-6, and IL-12) and increased the expression levels of anti-inflammatory cytokines (IL-10 and TGF-β). The hydrodynamic size of the L-Ag/R was 218 nm, which was maintained for more than one week in 10% serum. In an *in vivo* mouse model, co-delivery of rapamycin and MI antigens *via* intradermal injection of L-Ag/R induced DC maturation and increased the population of Treg cells. The immune tolerance ability of L-Ag/R inhibited unfavored cardiac remodeling and enhanced cardiac function. Infarct size and the amount of fibrosis after MI were almost 2 times lower than in the control samples. Unilamellar liposomes containing both MI tissue lysates and immune modulatory drugs effectively reduced the inflammatory response, resulting in less damage to heart tissue after MI.

Tumor-associated carbohydrate antigens (TACA) are glycan biomolecules covalently conjugated to lipids or proteins that are overexpressed on the surfaces of cancer cells. TACAs are innately weak immunogens by themselves, which limits vaccine development using them. Trabbic *et al.* synthesized AuNPs capped with β-1,3-Glucans and further functionalized with a MUC4 (mucin protein)-based glycopeptide antigen composed of MUC4 oligopeptides, a cathepsin-sensitive cleavage site, and a disaccharide antigen that is specifically overexpressed in tumor sites.[50] β-1,3-Glucans at the surface of the AuNPs can target the dectin-1 ligand on the surface of tumor macrophages. The average HD size of the AuNP-based NV was 40–50 nm. The NVs were delivered to macrophages and cathepsins, where they cleaved the specific sites of tumor antigens to recruit antigen-presenting cells and induce an immune response. In *in vivo* vaccination tests of MUC4 glycopeptides, the NVs were more than 10 times more effective at the cytokine stimulation level than a protein carrier, CRM197 (a non-toxic form of the diphtheria toxin).

3.2 Protein/gene delivery

Cytosolic delivery of proteins and genes is not an efficient process because their surface charge is negative under physiological conditions (*i.e.*, their isoelectric point (pI) is usually less than 7), which is very similar to the net surface charge of the cell membrane. Because of the increasing biological use and clinical need for protein drugs and gene editing techniques, researchers aim to enhance the delivery efficiency of proteins and genes.
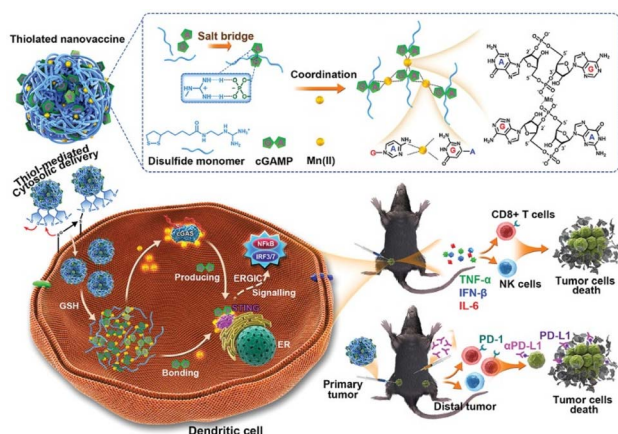

Fig. 6 Schematic representation of Mn–cGAMP NVs and the direct cytosolic delivery of cGAMP. This figure has been reproduced from ref. 48 with permission from [Wiley], copyright [2021].

Non-viral carriers are some of the most reliable vehicles because of their transience and lower chance of unexpected gene insertion compared with viral carriers.

Sarkar *et al.* reported a polyaspartic acid–based NP functionalized with aliphatic chains, amino-benzyl guanidinium, and quaternary ammonium moieties (Fig. 7).[51] The vehicle displayed a strong positive charge at the surface, resulting in nano-assembly *via* electrostatic interactions with both DNA and proteins. The colloidal stability of the nano-assembly was maintained even in DMEM for 24 hours. With an HD of 30 nm without a payload, the rhodamine-functionalized NPs were delivered into the cytosol *via* an energy-independent pathway. Cytosolic delivery of self-assembled protein (payload)–NP (polymer vehicle) composites was demonstrated under an 8 : 1 protein: polymer ratio. The polymer-based NP showed efficient transfection (>90%) for various cell types. Plasmid DNA with GFP was successfully delivered to various cell types, including KB, SHSY5Y, astrocytes, and progenitors. A higher expression level of GFP was achieved by polymeric nano-assembly, with less cytotoxicity and a shorter incubation time (2 h) than lipofectamine (12 h).

Physical methods for cytosolic delivery usually cause severe damage to the cell membrane.[52] A controlled fast acoustic flow was generated using a gigahertz-frequency (GHz) resonator that showed marginal deformation of the cell membrane and induced transiently improved intracellular delivery. This method has been used to increase the cellular uptake of drug molecules and nanomaterials with low cytotoxicity. Pan *et al.* reported a GHz acoustic resonator that can deliver various types of proteins into the cytosol of different cell lines. Using positively charged GFP and 400 mW GHz acoustic treatment for 20 min, cytosolic delivery of GFP was confirmed in HeLa cells with no noticeable cytotoxicity. However, higher than 400 mW GHz treatment induced severe cytotoxicity to HeLa cells. Cre recombinase is a cationic nuclease that targets LoxP recognition sites and specifically downregulates GFP expression in the transfected cell line. With Cre recombinase and GHz treatment, exogenous enzyme delivery was confirmed by GFP downregulation. For GHz treatment, cell-type and ATP-independent intracellular delivery were confirmed using various cell lines and endocytosis inhibitors.

Zhang *et al.* reported an NV composed of guanidinium-containing thiolated monomers, neoantigens, and agonists of toll-like receptor 9 (CpG-ODN).[53] The monomers connected and formed polysulfide NPs *via* self-assembly of antigens and CpG-ODN. The nanovaccines were loaded into cells *via* direct cytosolic delivery. The concentration of inflammation markers (IL-12, TNF-α) was increased after vaccination. Activation of bone marrow-derived dendritic cells and increasing T cell proliferation were obtained by cytosolic delivery of the nanovaccine in cultured cells. Subcutaneous injection of the nanovaccine in an *in vivo* mouse model led to maturation of more than 40% of dendritic cells and T cell activation in both the spleen and blood that was about ∼3 times higher than in the control condition. A dose of 5 vaccinations every 4 days improved the survival rate (80% for 3 months) and slowed the tumor growth rate. After 3 weeks of immunization, tumor-infiltrating lymphocytes were observed in the *in vivo* mouse model. Inhibiting the immune checkpoint through alph-PD1 and NV administration significantly retarded tumor growth *via* immune cell activation.

Mout *et al.* reported 10 nm arginine-terminated AuNPs for use as gene/protein carriers. The surface ligands were composed of arginine, ethylene glycol, and alkyl thiol.[54] The self-assembly of glutamate-terminated Cas9 protein and positively charged AuNPs occurred *via* electrostatic interaction. The hydrodynamic size of the nanoassembly was proportionally correlated to the number of glutamates on Cas9 (up to ∼475 nm). Their delivery mechanism showed that methyl-β-cyclodextrin treatment effectively blocked the cytosolic delivery of the AuNP carriers. Cholesterol-dependent membrane fusion was the main mechanism for delivery of the Cas9-AuNP nanoassembly. Fewer glutamates (0–10) caused the nanoassembly to not be delivered into the cytosol but instead to attach to the cell membrane. Using dye conjugation, cytosolic delivery of Cas9 was confirmed by cross-sectioned confocal images of the cells. Using the nanoassembly as a carrier for the CRISPR/Cas9 complex, human PTEN gene editing was performed in ∼30% for INDEL analysis.
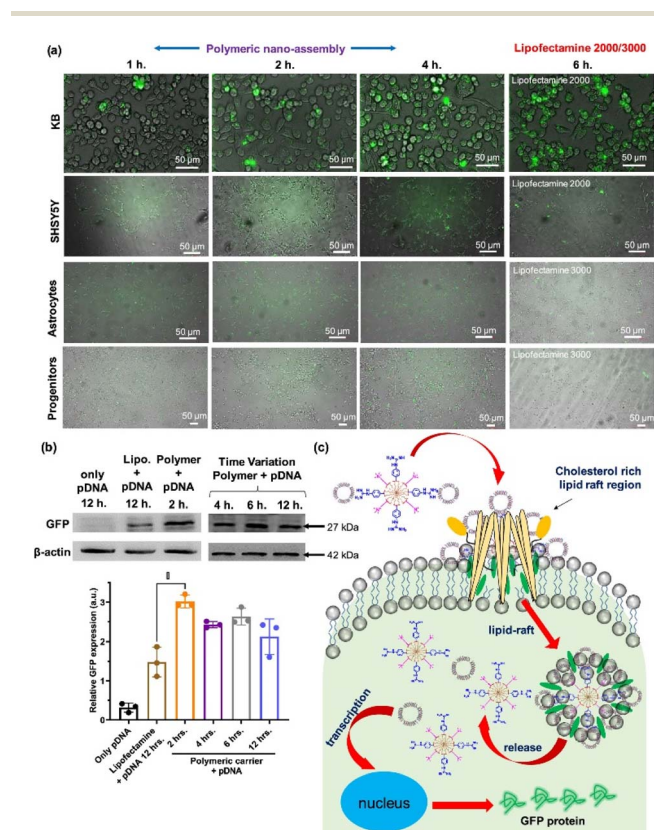

Fig. 7 Polyaspartic acid for efficient gene delivery carrier. (a) Various cell types were transfected with pDNA by co-incubation of either polymer-pDNA nano-assembly or lipofectamine-pDNA (b) western blot assay for quantitative estimation of GFP expression level of transfected cells (c) schematic representation of proposed cytosolic pDNA delivery mechanism *via* the nanoassembly. This figure has been reproduced from ref. 51 with permission from [American Chemical Society], copyright [2022].

Fig. 8 Cytosolic delivery of mitochondria specific peptide delivery with fluorous-tagging. This figure has been reproduced from ref. 56 with permission from [American Association for the Advancement of Science], copyright [2020].

3.3 Organelle-targeted imaging and enrichment

Mitochondria are the power plants for cells. Dysfunction of the mitochondria results in cancer and cardiovascular and auto-immune diseases. A functional protein/mAb nanoassembly for targeting mitochondria can be used as an organelle-specific drug. However, excessive functionalization of the proteins can alter their biological activity and delivery mechanism. Liew *et al.* synthesized a triphenylphosphine (TPP)-functionalized nanogel containing proteins or antibodies and successfully produced mitochondria-specific protein delivery.[55] Using glutathione (GSH)-triggered cleavable moieties of the nanogel, proteins can be delivered into the cytosol in a physiologically reducing environment. Western blots of the mitochondrial fraction and colocalization of MitoTracker using CLSM showed organelle-specific delivery of the nanogel. Not only GFP, but also RNase A were delivered into the cell cytosol by the nanogel carrier system. Colocalization of RNase A-FITC with Lysotracker showed endosomal escape followed by cytosolic delivery after 12 h. For RNase delivery, phenyl boric acid was conjugated on the nanogel to embed doxorubicin (DOX). Using reversible click chemistry between the phenyl boronic acid group and the aryl amine of the DOX, proteins and small-molecule drugs could be

Table 1 Cytosolic delivery strategies of nanoparticle-based delivery systems (β-gal: beta-galactosidase, HRP: horseradish peroxidase, Ctp: chymotrypsin, Trp: trypsin, GrA: granzyme-A, ALP: alakaline phosphatase, TNBC: triple-negative breast cancer)

Cytosolic delivery strategy	Target activatable/ specific moiety	Delivery cargo	Delivery mechnism	Disease/application	Ref.
Penetration	Tetra-guanidinium, pH responsive	Saporin, GFP, RNaseA	N/A	A549 xenograft mouse (lung cancer)	30
	Guanidyl-rich polymer	BSA-FITC, β-gal, HRP, Ctp, Trp	Energy dependent endocytosis	N/A	31
	Octaarginine, host–guest chemistry	GFP, β-gal, IgG	Endocytosis-independent (direct)	N/A	32
	Guanidinium, glutamate	Biotinylated GrA	Membrane fusion like (direct), lipid-raft mediated	Induce apoptosis	34
	Arginine, glutamate (E)	E-tagged GFP, Gr A	Membrane fusion like (direct), lipid-raft mediated	Apoptosis	33
Endosomal escape	DPA/Zn^{2+}	BSA and oligopeptides	Micropinocytosis-dependent and lipid-raft-associated	N/A	38
	ALP, phosphate	Phosphopeptides (D-(Lys-pTyr-Phe-Phe))	Caveolae-mediated, particle to nanofiber transition	N/A	39
	pH-responsive	HiBiT peptides	Endocytosis, destabilize endosomal membrane	N/A	40
Stimuli-sensitive	pH-sensitive polyamidoamine dendrimers	EGFP, SOD-FITC, RNase A-FITC, OVA-FITC, YFP, R-PE, β-gal	Lipid-raft mediated and clathrin-mediated endocytosis	4T1, HeLa, MT4, HepG2 cell	41
	$^1O_2$-cleavable linker	siRNA, antisense oligonucleotides, photosensitizer	NIR light irradiation	Cervix adenocarcinoma (mice bearing hell tumor)	42
	Perfluoropentane interior of PFC nanoemulsions	FTagged-protein (GFP, IgG, anti-β-tubulin)	Ultrasound, receptor (integrins)-mediated endocytosis and macropinocytosis	A549 cell, bitransgenic mouse model in which human HRas^{G12V} expressed	43
	Hypoxia-sensitive	RNase	Energy dependent endocytosis	4T1 TNBC model mouse	44
Fusogenic liposome	pH-responsive CHEMS/ DOPE liposome	HBsAg, CpG, oligonucleotides	pH-responsive membrane fusion	Hepatitis B virus	45
	DMPC/DSPE-PEG/ DOTAP	Iron oxide nanoparticle	Little bit of endocytosis and most of fusogenic liposome	N/A	46
	DOPE/DOTAP/DiR	eGFP-mRNA	Fusogenic liposome	N/A	47

Table 2 Nanomedicines for cytosolic delivery in the market or in the clinical trials

Cytosolic delivery methods	Product Name	Cargos	Disease (target)	Status	Ref.
Penetration	RT-002	Botulinum toxin A	Cervical dystonia	Completed	67
	AM-111	JNKI-1	Hearing loss	Phase III	68
Endosomal escapes	SNS01-T	siRNAs	Lymphoma, diffuse large B-cell, *etc.*	Phase I/II	69
Stimuli sensitive	AVB-620	Cy5 and Cy7	Breast cancer	Phase II	70
Liposome	Doxil	Doxorubicin hydrochloride	Acute myeloid leukemia, *etc.*	FDA approved(1995)	71

simultaneously loaded onto the nanogels. Then, the RNase and DOX could be released from the nanogels in the presence of both endogenous GSH and reactive oxygen species (ROS). The severe and synergistic cell cytotoxicity of the nanogel coloaded with RNase and DOX occurred in a concentration-dependent manner, whereas the GSH- and ROS-insensitive nanogel showed marginal cytotoxicity.

Peptides with target affinity and inhibition ability have been identified as drug candidates for undruggable proteins and diseases. Even with low toxicity and high selectivity, those peptides are susceptible to endogenous enzymes and exhibit a short half-life *in vivo*. Rong *et al.* synthesized fluorous-tagged peptide NPs that targeted mitochondria (Fig. 8).[56] Fluorinated alkyl thiols were covalently conjugated on peptides containing cysteine *via* disulfide bonds. After fluorination, the fluorinated peptides (F-P1) were assembled into a nanostructure in phosphate buffer conditions. F-P1 showed higher cytosolic delivery efficiency than the TAT- or octaarginine tagging methods. After intracellular delivery of F-P1, the intact P1 could be delivered *via* cleavage of disulfide bonds in the presence of endogenous glutathione. The delivery mechanism study revealed that intracellular delivery of F-P1 is an energy-dependent process that involves multiple endocytosis pathways. The stability to digestion of F-P1 was confirmed by coincubation of F-P1 (or TAT-P1) with chymotrypsin. Cell-type-independent cytosolic delivery was demonstrated. Fluorous-tagged KLAKLAKKLA-KLAK peptides (KLA), a proapoptotic peptide that induces apoptosis by mitochondrial membrane disruption, showed organelle-specific cytosolic delivery. Fluorous-tagged KLA also showed therapeutic efficacy in a xenograft tumor mouse model without a decrease in body weight.

Wen *et al.* synthesized a nucleus- or lysosome-targeted dye that induced photothermal therapy (PTT) under NIR laser irradiation. The structure of the dyes was based on PB09, which is a non-targeted dye with extremely short-lived excitons and rapid decay in a non-radiative pathway.[57] Deep-red emitting fluorescent dye and nucleus-targeting moieties (PKKKRKV peptides, nucleus localization sequences) were functionalized to synthesize the nucleus-targeted PTT dye (NucCR). For lysosomal targeting, morpholine groups were conjugated on the PTT dye (LysoCR). Nuclear colocalization of Hoechst 33342 and NucCR was confirmed by CLSM. Laser irradiation-dependent PTT efficacy was confirmed by a cell viability test that administered NucCR and its derivatives. Even though LysoCR induced only marginal cytotoxicity under laser irradiation, the neutral pH in the lysosome was confirmed by acridine orange dye labeling after LysoCR uptake and laser irradiation. Partial disruption of the lysosomal membrane could explain the pH equilibrium between lysosome and cytosol.

Not only mentioned above, nanomedicines for other subcellular organelles-targeting, including endoplasmic reticulum for cancer immunotherapy[58,59] and Golgi apparatus for curing liver fibrosis and cancer metastasis[60] have been researched extensively.

4 Conclusions and future perspectives

We summarized the recent progress in nanomedicine-mediated cytosolic delivery. Cytosolic delivery has been studied by researchers using various strategies, including CPPs, endosomal escape, stimuli-sensitive delivery, and FLs (Table 1). With these strategies, nanomedicines loaded with bioactive molecules have been applied to organelle-specific tagging, vaccine delivery for enhanced immunotherapy, and intracellular delivery of proteins and genes.

The surface chemistry of NPs can be optimized in relation to the intended therapeutic protein.[61–63] The flexible surface functionalization of the NP-based delivery platform allows NPs to be used as a model system that mimics specific biomolecules to study their delivery into the cytosol. Also, various proteins and genes can be delivered into specific cells and tissues by maximizing intracellular delivery strategies in conjunction with nanoparticles. These non-viral vehicles can have non-targeted and uncontrolled genetic alterations.[64] Depending on the composition of the cell membrane, membrane proteins and cholesterol can alter the intracellular delivery mechanisms of nanomedicines. Given that complexity and heterogeneity, NP surfaces have to be developed accurately to maximize their cytosolic delivery potential.

Upon cytosolic delivery, specific organelles and enzymes can be labeled and up- or downregulated, which has attracted great attention from researchers.[65,66] The efficacy of proteins can be enhanced using finely tuned NP-based delivery vehicles. The specific targeting moieties on the nanomedicines can easily isolate intracellular organelles with high purity and full functionality.

For further biomedical applications, the toxicity of NP-based delivery vehicles has to be carefully investigated and minimized. With proper choice of materials, surface modifications, and target specificity, cytosolic delivery mechanisms can be applied as efficient drug vehicles for human use. With the development of various cytosol delivery mechanisms, researchers need to choose and optimize them to meet their own goals. Some

cytosolic delivery methods have been clinically evaluated, approved, and used (Table 2).[67–71] For certain cases in clinical uses, combining those cytosolic delivery methods may be needed to achieve maximized cytosolic delivery. For example, FL, CPPs, and stimuli-sensitive can be combined those techniques on one nanomedicine to target specific cells and subcellular organelles with the highest efficiency. Because the next generation of cytosolic delivery methods is already being developed by researchers, we expect their clinical use to become a reality.

Conflicts of interest

The authors declare that they have no conflict of interest.

Acknowledgements

References

1 J. Shi, P. W. Kantoff, R. Wooster and O. C. Farokhzad, *Nat. Rev. Cancer*, 2017, **17**, 20–37.

2 Y. Min, J. M. Caster, M. J. Eblan and A. Z. Wang, *Chem. Rev.*, 2015, **115**, 11147–11190.

3 W. He, X. Xing, X. Wang, D. Wu, W. Wu, J. Guo and S. Mitragotri, *Adv. Funct. Mater.*, 2020, **30**, 1910566.

4 F. Scaletti, J. Hardie, Y.-W. Lee, D. C. Luther, M. Ray and V. M. Rotello, *Chem. Soc. Rev.*, 2018, **47**, 3421–3432.

5 D. E. Scott, A. R. Bayly, C. Abell and J. Skidmore, *Nat. Rev. Drug Discovery*, 2016, **15**, 533–550.

6 A. Blangy, H. A. Lane, P. d'Hérin, M. Harper, M. Kress and E. A. Nigg, *Cell*, 1995, **83**, 1159–1169.

7 D. Desplancq, G. Freund, S. Conic, A. P. Sibler, P. Didier, A. Stoessel, M. Oulad-Abdelghani, M. Vigneron, J. Wagner, Y. Mély, B. Chatton, L. Tora and E. Weiss, *Exp. Cell Res.*, 2016, **342**, 145–158.

8 J. Tu and A. C. H. Yu, *BME Front.*, 2022, **2022**, 9807347.

9 M. Chiper, K. Niederreither and G. Zuber, *Adv. Healthcare Mater.*, 2018, **7**, e1701040.

10 M. P. Murphy and R. C. Hartley, *Nat. Rev. Drug Discovery*, 2018, **17**, 865–886.

11 M. Themis, S. N. Waddington, M. Schmidt, C. von Kalle, Y. Wang, F. Al-Allaf, L. G. Gregory, M. Nivsarkar, M. Themis, M. V. Holder, S. M. Buckley, N. Dighe, A. T. Ruthe, A. Mistry, B. Bigger, A. Rahim, T. H. Nguyen, D. Trono, A. J. Thrasher and C. Coutelle, *Mol. Ther.*, 2005, **12**, 763–771.

12 S. Van Herck and B. G. De Geest, *Acta Pharmacol. Sin.*, 2020, **41**, 881–894.

13 A. Saminathan, M. Zajac, P. Anees and Y. Krishnan, *Nat. Rev. Mater.*, 2022, **7**, 355–371.

14 S. Du, S. S. Liew, L. Li and S. Q. Yao, *J. Am. Chem. Soc.*, 2018, **140**, 15986–15996.

15 J. Lv, Q. Fan, H. Wang and Y. Cheng, *Biomaterials*, 2019, **218**, 119358.

16 Y. Sun, S. Y. Lau, Z. W. Lim, S. C. Chang, F. Ghadessy, A. Partridge and A. Miserez, *Nat. Chem.*, 2022, **14**, 274–283.

17 J. Park, J. Nam, N. Won, H. Jin, S. Jung, S. Jung, S.-H. Cho and S. Kim, *Adv. Funct. Mater.*, 2011, **21**, 1558–1566.

18 J. Park, J. Lee, J. Kwag, Y. Baek, B. Kim, C. J. Yoon, S. Bok, S.-H. Cho, K. H. Kim, G. O. Ahn and S. Kim, *ACS Nano*, 2015, **9**, 6511–6521.

19 S. E. Park, N. S. El-Sayed, K. Shamloo, S. Lohan, S. Kumar, M. I. Sajid and R. K. Tiwari, *Bioconjugate Chem.*, 2021, **32**, 1898–1914.

20 Y. Jeong, S. Jin, L. Palanikumar, H. Choi, E. Shin, E. M. Go, C. Keum, S. Bang, D. Kim, S. Lee, M. Kim, H. Kim, K. H. Lee, B. Jana, M.-H. Park, S. K. Kwak, C. Kim and J.-H. Ryu, *J. Am. Chem. Soc.*, 2022, **144**, 5503–5516.

21 M. Green and P. M. Loewenstein, *Cell*, 1988, **55**, 1179–1188.

22 G. Guidotti, L. Brambilla and D. Rossi, *Trends Pharmacol. Sci.*, 2017, **38**, 406–424.

23 G. Feger, B. Angelov and A. Angelova, *J. Phys. Chem. B*, 2020, **124**, 4069–4078.

24 S. He, J. Fang, C. Zhong, F. Ren and M. Wang, *Acta Biomater.*, 2022, **140**, 149–162.

25 N. M. Hamelmann, J.-W. D. Paats and J. M. J. Paulusse, *ACS Macro Lett.*, 2021, **10**, 1443–1449.

26 Y.-B. Hu, E. B. Dammer, R.-J. Ren and G. Wang, *Transl. Neurodegener.*, 2015, **4**, 18.

27 M. Akishiba, T. Takeuchi, Y. Kawaguchi, K. Sakamoto, H. H. Yu, I. Nakase, T. Takatani-Nakase, F. Madani, A. Gräslund and S. Futaki, *Nat. Chem.*, 2017, **9**, 751–761.

28 A. Erazo-Oliveras, K. Najjar, L. Dayani, T. Y. Wang, G. A. Johnson and J. P. Pellois, *Nat. Methods*, 2014, **11**, 861–867.

29 Z. Gu, A. Biswas, M. Zhao and Y. Tang, *Chem. Soc. Rev.*, 2011, **40**, 3638–3655.

30 L. Fu, X. Hua, X. Jiang and J. Shi, *Nano Lett.*, 2022, **22**, 111–118.

31 J. Lv, E. Tan, Y. Wang, Q. Fan, J. Yu and Y. Cheng, *J. Controlled Release*, 2020, **320**, 412–420.

32 H. Kitagishi, M. Jiromaru and N. Hasegawa, *ACS Appl. Bio Mater.*, 2020, **3**, 4902–4911.

33 R. Mout, M. Ray, T. Tay, K. Sasaki, G. Yesilbag Tonga and V. M. Rotello, *ACS Nano*, 2017, **11**, 6416–6421.

34 D. C. Luther, Y. W. Lee, H. Nagaraj, V. Clark, T. Jeon, R. Goswami, S. Gopalakrishnan, S. Fedeli, W. Jerome, J. L. Elia and V. M. Rotello, *ACS Nano*, 2022, **16**, 7323–7330.

35 J. Váňová, A. Hejtmánková, M. H. Kalbáčová and H. Španielová, *Materials*, 2019, **12**, 2671.

36 A. Nasrolahi Shirazi, R. K. Tiwari, D. Oh, B. Sullivan, K. McCaffrey, D. Mandal and K. Parang, *Mol. Pharm.*, 2013, **10**, 3137–3151.

37 H. Jing, M. Pálmai, B. Saed, A. George, P. T. Snee and Y. S. Hu, *Nanoscale*, 2021, **13**, 5519–5529.

38 L. Ren, J. Lv, H. Wang and Y. Cheng, *Angew. Chem., Int. Ed. Engl.*, 2020, **59**, 4711–4719.

39 H. He, J. Guo, J. Xu, J. Wang, S. Liu and B. Xu, *Nano Lett.*, 2021, **21**, 4078–4085.

40 M. A. Beach, S. L. Y. Teo, M. Z. Chen, S. A. Smith, C. W. Pouton, A. P. R. Johnston and G. K. Such, *ACS Appl. Mater. Interfaces*, 2022, **14**, 3653–3661.

41 S. Zhang, J. Lv, P. Gao, Q. Feng, H. Wang and Y. Cheng, *Nano Lett.*, 2021, **21**, 7855–7861.

42 L. Chen, G. Li, X. Wang, J. Li and Y. Zhang, *ACS Nano*, 2021, **15**, 11929–11939.

43 J. N. Sloand, T. T. Nguyen, S. A. Zinck, E. C. Cook, T. J. Zimudzi, S. A. Showalter, A. B. Glick, J. C. Simon and S. H. Medina, *ACS Nano*, 2020, **14**, 4061–4073.

44 X. Si, S. Ma, Y. Xu, D. Zhang, N. Shen, H. Yu, Y. Zhang, W. Song, Z. Tang and X. Chen, *J. Controlled Release*, 2020, **320**, 83–95.

45 F. Hu, H. Yue, T. Lu and G. Ma, *J. Controlled Release*, 2020, **324**, 460–470.

46 F. Chen, M. Bian, M. Nahmou, D. Myung and J. L. Goldberg, *RSC Adv.*, 2021, **11**, 35796–35805.

47 M. Hoffmann, N. Hersch, S. Gerlach, G. Dreissen, R. Springer, R. Merkel, A. Csiszár and B. Hoffmann, *Int. J. Mol. Sci.*, 2020, **21**, 2244.

48 C. Chen, Y. Tong, Y. Zheng, Y. Shi, Z. Chen, J. Li, X. Liu, D. Zhang and H. Yang, *Small*, 2021, **17**, e2006970.

49 S. P. Kwon, B.-H. Hwang, E.-H. Park, H. Y. Kim, J.-R. Lee, M. Kang, S. Y. Song, M. Jung, H. S. Sohn, E. Kim, C. W. Kim, K. Y. Lee, G. C. Oh, E. Choo, S. Lim, Y. Chung, K. Chang and B.-S. Kim, *Small*, 2021, **17**, 2101207.

50 K. R. Trabbic, K. A. Kleski and J. J. Barchi Jr, *ACS Bio Med Chem Au*, 2021, **1**, 31–43.

51 A. K. Sarkar, K. Debnath, H. Arora, P. Seth, N. R. Jana and N. R. Jana, *ACS Appl. Mater. Interfaces*, 2022, **14**, 3199–3206.

52 S. Pan, T. Jeon, D. C. Luther, X. Duan and V. M. Rotello, *ACS Appl. Mater. Interfaces*, 2020, **12**, 15823–15829.

53 D. Zhang, Z. Lin, M. Wu, Z. Cai, Y. Zheng, L. He, Z. Li, J. Zhou, L. Sun, G. Chen, Y. Zeng, J. Li, J. Liu, H. Yang and X. Liu, *Adv. Sci.*, 2021, **8**, 2003504.

54 R. Mout, M. Ray, G. Yesilbag Tonga, Y. W. Lee, T. Tay, K. Sasaki and V. M. Rotello, *ACS Nano*, 2017, **11**, 2452–2458.

55 S. S. Liew, J. Zhou, L. Li and S. Q. Yao, *Chem. Commun.*, 2021, **57**, 3215–3218.

56 G. Rong, C. Wang, L. Chen, Y. Yan and Y. Cheng, *Sci. Adv.*, 2020, **6**, eaaz1774.

57 Y. Wen, H. H. McGarraugh, C. L. Schreiber and B. D. Smith, *Chem. Commun.*, 2020, **56**, 6977–6980.

58 H. Deng, Z. Zhou, W. Yang, L.-s. Lin, S. Wang, G. Niu, J. Song and X. Chen, *Nano Lett.*, 2020, **20**, 1928–1933.

59 C. Ghosh, A. Nandi and S. Basu, *Nanoscale*, 2019, **11**, 3326–3335.

60 H. Li, P. Zhang, J. Luo, D. Hu, Y. Huang, Z.-R. Zhang, Y. Fu and T. Gong, *ACS Nano*, 2019, **13**, 9386–9396.

61 S. Ashraf, J. Park, M. A. Bichelberger, K. Kantner, R. Hartmann, P. Maffre, A. H. Said, N. Feliu, J. Lee, D. Lee, G. U. Nienhaus, S. Kim and W. J. Parak, *Nanoscale*, 2016, **8**, 17794–17800.

62 J. Park, Y. Kuo, J. Li, Y.-L. Huang, E. W. Miller and S. Weiss, *J. Phys. Chem. Lett.*, 2019, **10**, 3906–3913.

63 J. Nam, N. Won, J. Bang, H. Jin, J. Park, S. Jung, S. Jung, Y. Park and S. Kim, *Adv. Drug Delivery Rev.*, 2013, **65**, 622–648.

64 A. S. Piotrowski-Daspit, C. Barone, C. Y. Lin, Y. Deng, D. Wu, T. C. Binns, E. Xu, A. S. Ricciardi, R. Putman, A. Garrison, R. Nguyen, A. Gupta, R. Fan, P. M. Glazer, W. M. Saltzman and M. E. Egan, *Sci. Adv.*, 2022, **8**, eabo0522.

65 J. A. Kretzmann, D. C. Luther, C. W. Evans, T. Jeon, W. Jerome, S. Gopalakrishnan, Y.-W. Lee, M. Norret, K. S. Iyer and V. M. Rotello, *J. Am. Chem. Soc.*, 2021, **143**, 4758–4765.

66 S. N. Tammam, H. M. E. Azzazy and A. Lamprecht, *J. Controlled Release*, 2016, **229**, 140–153.

67 J. Jankovic, D. Truong, A. T. Patel, A. Brashear, M. Evatt, R. G. Rubio, C. K. Oh, D. Snyder, G. Shears and C. Comella, *Mov. Disord. Clin. Pract.*, 2018, **5**, 273–282.

68 M. St Peter, D. E. Brough, A. Lawrence, J. Nelson-Brantley, P. Huang, J. Harre, A. Warnecke and H. Staecker, *Front. Bioeng. Biotechnol.*, 2022, **10**, 892969.

69 J. A. Lust, C. Barranco, S. Z. Usmani, F. van Rhee, M. Hamadani, J. Thompson, C. A. Taylor, R. Dondero, L. J. Browne, D. Siegel and W. I. Bensinger, *Blood*, 2013, **122**, 1950.

70 M. Miampamba, J. Liu, A. Harootunian, A. J. Gale, S. Baird, S. L. Chen, Q. T. Nguyen, R. Y. Tsien and J. E. González, *Theranostics*, 2017, **7**, 3369–3386.

71 D. Goren, A. Gabizon and Y. Barenholz, *Biochim. Biophys. Acta, Biomembr.*, 1990, **1029**, 285–294.